

## Notes

## Spectral Modulation and Exciton Migration in Thiophene-Based Polybenzobisoxazole Random Copolymers with Donor–Acceptor Architectures

Yan Chen, Shanfeng Wang,<sup>†</sup> Qixin Zhuang, Xinxin Li, Pingping Wu, and Zhewen Han\*

Key Laboratory for Ultrafine Materials of Ministry of Education, School of Materials Science and Engineering, East China University of Science and Technology, Shanghai 200237, China

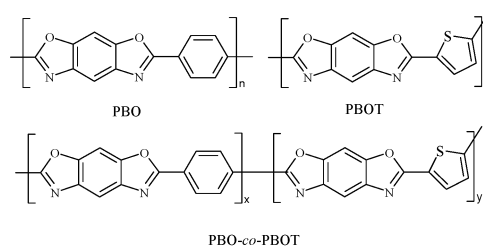
Received July 12, 2005

Revised Manuscript Received September 14, 2005

The conjugated rigid-rod polybenzobisoxazoles are a type of high-performance polymer with robust high-temperature resistance, photochemical and electrochemical stability, n-type dopability, and solution processability.<sup>1–4</sup> Jenekhe and co-workers<sup>3</sup> made systematic pioneering efforts on polybenzobisoxazoles as efficient electron transport materials and applied chemical tailoring to achieve desirable properties. Generally, chemical tailoring includes (1) the introduction of heterocycles into the polymer backbone to increase the electron cloud density and (2) the copolymerization of strong electron-donor and electron-acceptor moieties to reduce the band gap with an intrachain charge-transfer mechanism.<sup>5</sup> Thiophene-based systems have been investigated to reduce the band gap because of their stability and structural versatility.<sup>6</sup> Replacement of the phenyl moiety by the electron-rich thiophene moiety in benzobisthiazole model compounds was found to enhance the third-order optical susceptibility  $\chi^{(3)}$ .<sup>7</sup> Poly-(2,5-thienylbenzobisoxazole) (PBOT) was first synthesized as a liquid crystalline polymer, and its nonlinear backbone secondary structure could increase tractability and solubility compared to poly(*p*-phenylenebenzobisoxazole) (PBO).<sup>8</sup> The unrevealed photoluminescence properties of PBOT attracted our attention because the emitting color can be adjusted by changing the content of the narrow band gap, electron-donating thiophene ring based on the energy-transfer principle, considering the benzobisoxazole moiety is an electron acceptor.

In this paper, a series of thiophene-based polybenzobisoxazole copolymers poly(1,4-phenylenebenzobisoxazole-co-thienylbenzobisoxazole) (PBO-co-PBOT) with different ratios of thiophene and phenylene moieties have been synthesized and characterized. The interplay between morphology, donor–acceptor architecture, and photophysical properties of the copolymers as well as their parent polymers will be discussed using wide-angle X-ray diffraction (WAXD), UV–vis absorption, photo-

luminescence (PL) spectra, electrochemical cyclic voltammetry (CV), and time-resolved PL decay dynamics. The role of exciton migration and trapping in controlling emission will be emphasized.



PBO-co-PBOT copolymers with different PBOT contents were prepared via polycondensation from newly synthesized 2,4-diamino-1,5-benzenediol (DABDO) dihydrochloride with two diacids: terephthalic acid (TA) and 2,5-thiophene diacid (TDA) in freshly prepared poly-(phosphoric acid) (PPA). The polycondensation and polymer purification were similar to the procedures for other polybenzobisoxazoles described previously.<sup>4</sup> The copolymers CO5, -15, -25, -30, and -50 are named after the feed molar content of TDA in two diacids ranging from 5 to 50%. Intrinsic viscosities  $[\eta]$  of the polymers, measured at 30 °C in methanesulfonic acid (MSA), are 24.5, 5.49, 1.9, 1.56, 3.85, and 1.53 dL g<sup>-1</sup> for PBO, CO5 to CO30, and PBOT, respectively. For CO30, <sup>1</sup>H NMR (D<sub>2</sub>SO<sub>4</sub>, ppm):  $\delta$  = 8.7–8.8 (16H), 8.5–8.6 (10H), 8.24 (3H). FTIR (free-standing film, cm<sup>-1</sup>): 1585, 1363, 1626, 1113, 1493, 1412, 1058, 1213, 909, 740. Thin films were fabricated by Jenekhe's method,<sup>9</sup> i.e., spin-coating of the polymer solution in nitromethane/AlCl<sub>3</sub> with a polymer concentration of ~3 wt % onto synthetic silica substrates for optical characterizations or strictly cleaned indium tin oxide (ITO) substrates for electrochemical CV. The thin films were dried at 80 °C in a vacuum oven for 12 h after complete decomplexation in deionized water.

Thermogravimetric analysis (TGA) obtained in flow nitrogen at a heating rate of 10 °C/min shows that all the polymers start to decompose at 600–700 °C. No weight loss was found between 200 and 260 °C, indicating no residual PPA in the polymers. In agreement with the earlier report on PBOT, the introduction of thiophene does not weaken much the thermal stability of the polymers despite the lower inherent viscosities, which result from possibly lower molecular weights and also the nonlinearity introduced into the polymer backbone by the thiophene heterocycle with an exocyclic bond angle of 148°.<sup>8</sup>

All the polymers herein are lyotropic as indicated by stir opalescence in polycondensation despite the nonlinearity in thiophene-containing polymers. WAXD patterns of all the polymers in Figure 1 have two major diffraction peaks around  $2\theta$  = 16° (~0.55 nm, labeled as peak A) and 26° (~0.35 nm, peak B). The periodicity

<sup>†</sup> Current address: Mayo Clinic College of Medicine, Rochester, MN 55901.

\* Corresponding author: Tel +8621-64253060; fax +8621-64233269, e-mail zhwhan@ecust.edu.cn.

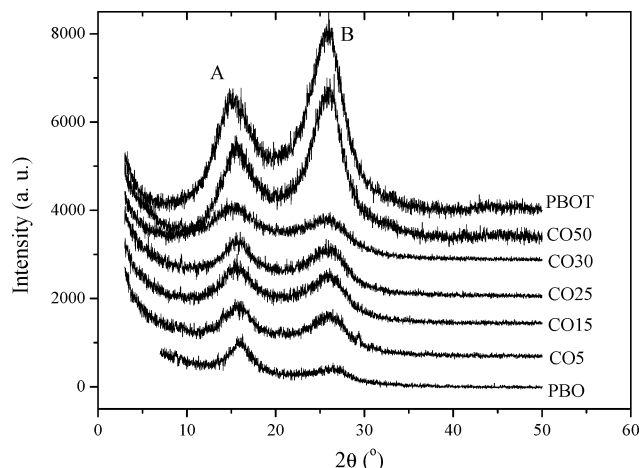


**Figure 1.** Wide-angle X-ray diffraction patterns of PBO, PBOT, and PBO-PBOT copolymers.

for peaks A and B stands for “side-by-side” distance on (200) plane and “face-to-face” distance on (010) plane between two neighboring polymer chains, respectively.<sup>10</sup> With increasing PBOT content, the “side-by-side” and “face-to-face” distances increase slightly from 0.550 to 0.596 nm and 0.346 to 0.352 nm, respectively. The result suggests that the heterocycles of PBO and PBOT are on the same plane with a small dihedral angle, and the monoclinic crystalline system<sup>10</sup> of PBO most likely remains.

The optical absorption properties have been investigated in both MSA dilute solution and thin film with the spectra shown in Figure 2. A general trend of red shift of absorption edge ( $\lambda_{\text{onset}}$ ) with the increase of thiophene content can be observed, and the energy gap determined from  $\lambda_{\text{onset}}$  in dilute solution decreases from 2.79 eV for PBO to 2.47 eV for PBOT. Besides two major peaks of PBO at 400 and 427 nm, a small shoulder appears at a longer wavelength of  $\sim 451$  nm, and it progressively grows with increasing PBOT content. Meanwhile, the PBO absorption peak at  $\sim 405$  nm diminishes and disappears eventually. The absorption spectra of thin films in Figure 2b are essentially similar to those of polymer solutions with the same trend except that they are less resolved with broadened bandwidth. The similarity, however, arises from different origins because the protonation effect in MSA solution and strong interchain interactions in the solid state cause the same bathochromic shift in the absorption of polybenzoxazoles when compared to that of a neutral isolated chain.<sup>4i,j</sup>

The thin film electrochemical energy gap  $E_g^{\text{el}}$  varies from 2.93 eV for PBO to 2.57 eV for PBOT, and the energy gap  $E_g^{\text{opt}}$  from  $\lambda_{\text{onset}}$  in Figure 2b is from 2.76 to 2.44 eV, showing the consistency within experimental errors. PBOT's lower band gap can be ascribed to the weaker steric hindrance between thiophene ring and benzobisoxazole heterocycle than that between benzene ring and heterocycle. An easier rotation consequently broadens the conjugation range and brings better electronic delocalization.<sup>11</sup> In addition, the thiophene moiety is a better electron donor than the phenylene moiety. The onset redox potentials and the calculated HOMO (highest occupied molecular orbital) and LUMO (lowest unoccupied molecular orbital) energy parameters<sup>12</sup> are tabulated in Table 1. LUMO energy changes little while HOMO energy is more sensitive to the thiophene content, as also reported for the copolymers of fluorene and thiophene.<sup>13a-c</sup>

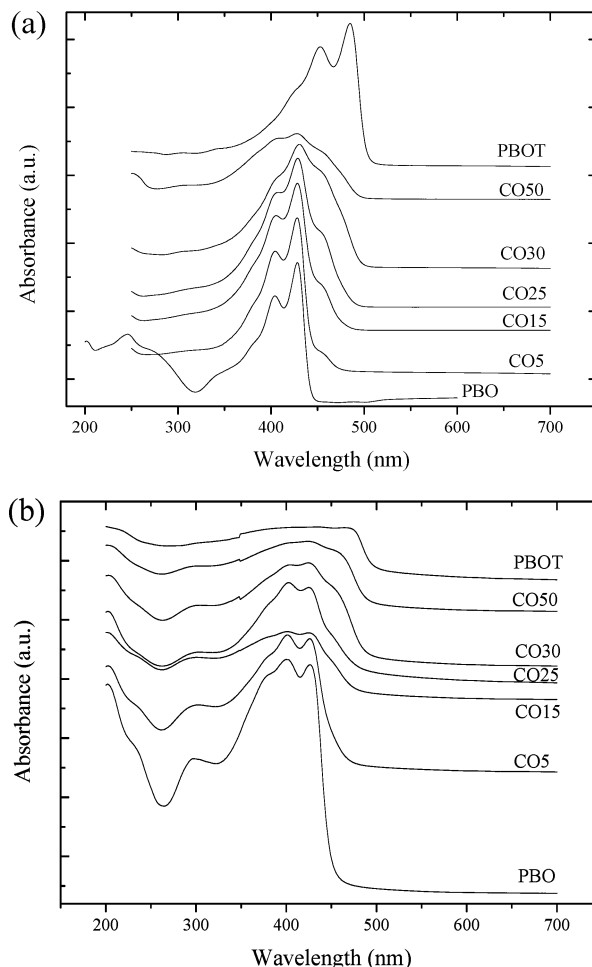


**Figure 2.** Absorption spectra of PBO, PBOT, and their copolymers (a) in MSA dilute solution (0.00044 g dL<sup>-1</sup>) and (b) thin films.

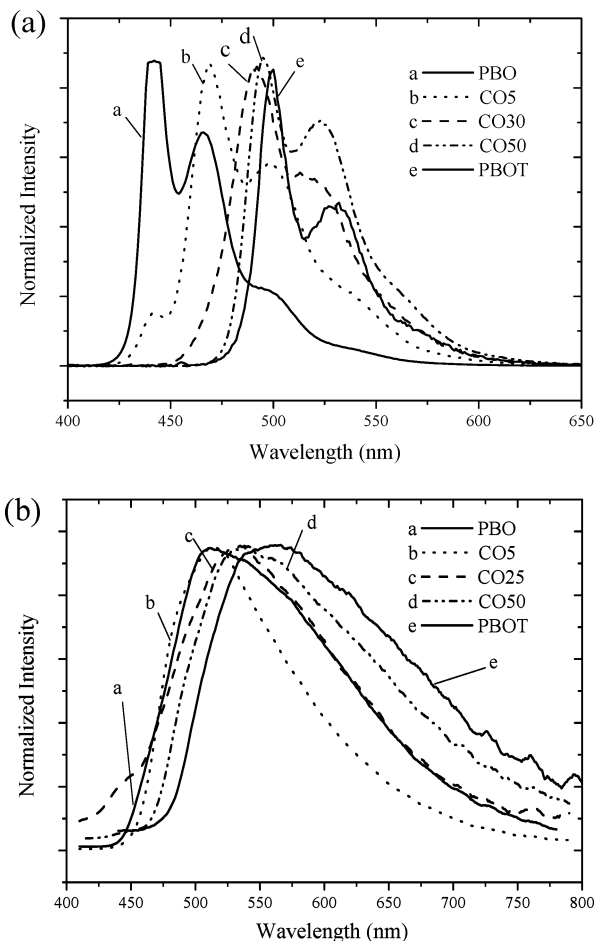
The PL emission spectra of the dilute solutions in MSA (0.00044 g dL<sup>-1</sup>) in Figure 3a are narrow peaks with vibronic structure to show singlet intrachain exciton in the absence of excimer or aggregate. The emission maxima (469 nm for CO5) in Figure 3a are apparently red-shifted from that for PBO (439 nm) despite that the absorption maxima ( $\lambda_{\text{max}}$ ) of the copolymer solutions are identical with that of PBO solution (429 nm). Furthermore, no emission from PBO can be observed while a longer wavelength emission from PBOT is dominant when the PBOT content is larger than 5%, showing that an efficient exciton migration and trapping<sup>13,14</sup> occurs from higher band gap PBO to lower band gap PBOT upon excitation. Thereby, the Stokes shifts between the emission and absorption maxima for these copolymers are much higher (40–65 nm and 0.25–0.28 eV, respectively) than 10 nm (0.07 eV) for PBO and 15 nm (0.08 eV) for PBOT. Such a larger Stokes shift induced by exciton migration (Figure S4 in Supporting Information) is reminiscent of a similar case in poly(*p*-phenylenebenzobisoxazole)-copoly(2,5-benzoxazole) (PBO-ABPBO) with ABPBO as a higher band gap component and PBO as a lower one.<sup>4d,e</sup> It is also interesting to note that  $\lambda_{\text{onset}}$  increases at the same pace as emission maximum by jumping to a plateau at a PBOT content of  $\sim 30\%$ , as seen in Figure S4.

Color tuning can be also observed for the polymer films in Figure 3b. However, the thin film PL spectra

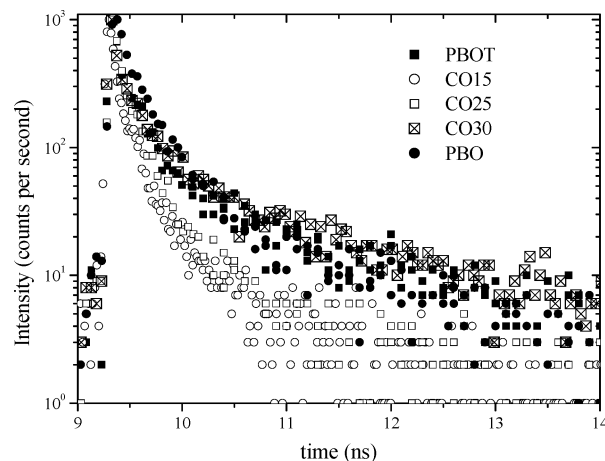
**Table 1. Absorption Data, Electrochemical Energy Gap, and Time-Resolved PL Decay Dynamics Parameters of Polymer Thin Films**

	absorption $\lambda$ (nm)			$\lambda_{\text{onset}}$ (nm)	$E_{\text{g}}^{\text{opt}}$ (eV)	$E_{\text{g}}^{\text{el}}$ (eV)	$E_{\text{ox}}$ (V)	$E_{\text{red}}$ (V)	$E_{\text{HOMO}}$ (eV)	$E_{\text{LUMO}}$ (eV)	$\tau_1$ , ns (%)	$\tau_2$ , ns (%)	$\lambda_{\text{det}}$ (nm)
	$\lambda_1$	$\lambda_2$	$\lambda_3$										
PBO	400*	427		450	2.76	2.93	1.65	-1.28	-6.05	-3.12	0.28 (33.8)	1.40 (66.2)	507
CO5	401*	426		478	2.60	2.78	1.51	-1.27	-5.91	-3.13	0.17 (33.5)	0.65 (66.5)	508
CO15	401*	425		493	2.51	2.78	1.48	-1.30	-5.88	-3.10	0.12 (43.0)	0.49 (57.0)	512
CO25	402*	425	451 <sup>a</sup>	494	2.51	2.71	1.46	-1.25	-5.86	-3.15	0.31 (100)		532
CO30	405*	424	455 <sup>a</sup>	495	2.50	2.63	1.40	-1.23	-5.80	-3.17	0.44 (16.7)	2.09 (83.3)	530
CO50		424*	456 <sup>a</sup>	499	2.48	2.61	1.37	-1.24	-5.77	-3.16	0.54 (31.1)	2.68 (68.9)	538
PBOT		432*	464	506	2.44	2.57	1.35	-1.22	-5.75	-3.18	0.32 (17.0)	1.57 (83.0)	560

<sup>a</sup> Shoulder peak; \*maximum absorption wavelength  $\lambda_{\text{max}}$ ;  $\lambda_{\text{onset}}$  = onset of absorption edge;  $E_{\text{g}}^{\text{opt}}$  = energy gap determined from  $\lambda_{\text{onset}}$ ;  $E_{\text{g}}^{\text{el}}$  = electrochemical energy gap;  $E_{\text{ox}}$  = onset of oxidation;  $E_{\text{red}}$  = onset of reduction. Time-resolved PL decay dynamics were determined at  $\lambda_{\text{det}}$  for polymer films excited at 370 nm.  $E_{\text{HOMO}}$  and  $E_{\text{LUMO}}$  were calculated by  $E_{\text{HOMO}} = -e(E_{\text{ox}} + 4.4)$  (eV) and  $E_{\text{LUMO}} = -e(E_{\text{red}} + 4.4)$  (eV).<sup>12</sup>

**Figure 3.** PL emission spectra of PBO, PBOT, and their copolymers (a) in dilute solution in MSA dilute solution (0.000 44 g dL<sup>-1</sup>) and (b) thin films.

are broad, featureless, and significantly red-shifted by 40–70 nm compared to those of the corresponding solutions in Figure 3a. Large Stokes shifts range from 110 nm (0.67 eV) to 144 nm (0.80 eV). The emission maxima vary little when excited at 371, 432, and 460 nm, as Förster energy transfer to the lowest energy segments is efficient and proceeds much faster than radiative relaxation. It should be pointed out that the original spectra (not shown) of CO5–25 before normalization as in Figure 3b are distinguished from those of PBO, PBOT, and copolymers with PBOT content greater than 30% by higher intensities and narrower bandwidth. The PL intensity drops gradually when increasing the PBOT content further since thiophene-based copolymers normally suffer low quantum efficiency due

**Figure 4.** Time-resolved PL decay dynamics of PBO, PBOT, and their copolymers excited at 370 nm.

to sulfur atom's heavy element effect.<sup>13a–c</sup> The exciton migration and trapping mechanism can be also used to interpret thin film emission spectra; however, it is more complicated than that in dilute solution because the interchain excimer or aggregate formed in solid state causes low quantum yield and inhomogeneous broadening due to the polybenzazoles' relatively planar geometries and sandwich-type cofacial packing distances of order 3–4 Å.<sup>3f</sup> Here we use the term "aggregate" to represent possibly coexisting excimers and ground-state aggregates with two or more chromophores.<sup>15</sup> Two lower band gap aggregation sites of PBO and PBOT in the solid state are involved besides the isolated chains, which normally exist in dilute fluid or solid solution. Both effects of *spatial confinement* and *chromophore size* play roles for making isolated shorter PBOT chromophores in the copolymers with low PBOT contents.<sup>3i,4e,f,16</sup> Once the chromophores are excited, excitons will be trapped either in the isolated PBOT chromophores or in PBO aggregate sites, depending on which one has a lower  $\pi-\pi^*$  transition, if they are not quenched in a nonemissive way. When the PBOT content is higher than 30%, PBOT aggregate sites will trap all the excitons fast and efficiently, as reflected in Figure 3b. On the other hand, the energy level structures for the different conjugated segments can be hybridized and integrated in random copolymers when neither component is absolutely dominant.<sup>13b</sup>

The time-resolved PL decay dynamics of PBO, PBOT, and their copolymer films depicted in Figure 4 further support the discussions above. The lifetimes and their corresponding amplitudes obtained from the best fit are listed in Table 1. The PL decay dynamics of the



copolymers with PBOT contents greater than 30% can be described satisfactorily by a biexponential decay mechanism. The multiple lifetimes of the polymers suggest the existence of more than one excited-state species or the occurrence of various excited-state processes.<sup>3i,17</sup> Coupled with the emission spectral broadening and large Stokes shift, the components with longer lifetimes in the solid state normally evidence aggregate formation.<sup>3i,17</sup> PBO and PBOT have similar decay lifetimes with a difference that the amplitude of the longer lifetime of PBOT (1.57 ns, 83.0%) is larger than that of PBO (1.40 ns, 66.2%). The faster component of the film PL decay corresponding to the singlet excitonic emission has lifetimes of only several hundred picoseconds, in agreement with the earlier reports on polybenzazole solutions and films.<sup>2–4</sup> The longer lifetime  $\tau_2$  (1.4–2.68 ns) is around 5 times the corresponding shorter lifetime  $\tau_1$ , and it is dominant in PBO, PBOT, and their copolymers with PBOT composition higher than 30%, confirming the aggregate formation and exciton migration to aggregate sites together with PL analysis above. The increasing amplitude of  $\tau_2$  with lower band gap PBOT content perfectly agrees with an opposite trend when increasing the nonconjugated (or higher band gap) content in polybenzazole-based rod-coil copolymers,<sup>3i,4f</sup> in which the *spatial confinement* effect reduces the interchain interaction of polybenzazoles using flexible nonconjugated segments. The longer lifetime of the aggregate-like emission suggests that the associated transition is less allowed than the corresponding intrachain transition; consequently, it will suppress the PL efficiency in films.<sup>15,17</sup>

Interestingly, the PL decay dynamics of copolymers with PBOT contents less than 30% are notably different from the others, including both PBO and PBOT with faster decay profiles as shown in Figure 4. Although both CO5 and CO15 can be still expressed by biexponential decay profiles, their two decay lifetimes are both around several hundred picoseconds with 0.65 ns (66.5%) and 0.49 ns (57.0%) as  $\tau_2$ , respectively. The latter 0.49 ns is even shorter than  $\tau_1$  (0.54 ns) of CO50. Therefore, the possibility that the longer lifetime components of CO5 and CO15 are from the aggregates can be safely ruled out. For CO25, the best fit of the decay profile even gives a singlet exciton transition with  $\tau_1 = 0.31$  ns. As discussed for their higher emission intensity and narrower emission bandwidth, the fast and efficient exciton migration process occurs from higher band gap chromophoric segments to isolated lower band gap PBOT chromophores in CO5–25. This explanation also offers a valid method to design quantum-well-like lower band gap traps in a bulk of higher band gap aggregates to achieve desirable emitting color with higher efficiency through copolymerization.<sup>16</sup>

In summary, a series of random copolymers (PBO-co-PBOT) with different PBOT contents have been synthesized, characterized, and used to demonstrate the spectral modulation, exciton migration, and trapping in both dilute solution and thin film. The copolymers with thiophene component have similar excellent thermal stability and ordered chain packing despite the lower intrinsic viscosities compared to PBO. The photophysical properties of these polymers in dilute solution show the band gap modulation by *intrachain* exciton migration and trapping. Two additional cases have to be considered for copolymer thin films as (1) aggregate formation responsible for the inhomogeneously broadened emis-

sion peak with a low quantum yield and (2) the hybridization and integration of the energy level structures of the two components in the random copolymers at PBOT contents higher than 30%. Nevertheless, exciton migration and trapping still occurs when a small amount of lower band gap PBOT segments (<30%) are spatially confined in higher band gap PBO aggregates to avoid either PBO or PBOT aggregate-like emission, supported by a fairly higher emission intensity with much narrower bandwidth without the longer lifetime component. Based on the current understanding, studies are being performed to achieve high quantum efficiency from the blends or copolymers consisting of polybenzazoles. The preliminary results on PBO(95%)/PBOT(5%) blend show a much enhanced quantum yield of photophysical processes to indicate efficient *interchain* energy transfer.

**Acknowledgment.** This research was supported by the “863” project of the National Science and Technology Department of China. The number of the financial item is 2002AA305109.

**Supporting Information Available:** Detailed experimental section and scheme for synthesis; FTIR, TGA, PL excitation spectra, and three characteristic wavelengths vs copolymer composition; tables of data of the polymer physical properties, WAXD patterns (Figure 1), and absorption spectra (Figure 2). This material is available free of charge via the Internet at <http://pubs.acs.org>.

## References and Notes

- Wolfe, J. F. In *Encyclopedia of Polymer Science and Technology*, 2nd ed.; Mark, H. F., Kroschmitz, J. I., Eds.; Wiley: New York, 1988; Vol. 11, pp 601–635.
- So, Y.-H.; Zaleski, J. M.; Murllick, C.; Ellaboudy, A. *Macromolecules* **1996**, *29*, 2783.
- (a) Osaheni, J. A.; Jenekhe, S. A.; Perlstein, J. *J. Phys. Chem.* **1994**, *98*, 12727. (b) Osaheni, J. A.; Jenekhe, S. A.; Perlstein, J. *Appl. Phys. Lett.* **1994**, *64*, 3112. (c) Osaheni, J. A.; Jenekhe, S. A. *Macromolecules* **1993**, *26*, 4726. (d) Osaheni, J. A.; Jenekhe, S. A. *Chem. Mater.* **1992**, *4*, 1282. (e) Osaheni, J. A.; Jenekhe, S. A. *Chem. Mater.* **1994**, *6*, 1906. (f) Jenekhe, S. A.; Osaheni, J. A. *Science* **1994**, *265*, 765. (g) Osaheni, J. A.; Jenekhe, S. A. *Chem. Mater.* **1995**, *7*, 672. (h) Jenekhe, S. A. *Adv. Mater.* **1995**, *7*, 309. (i) Osaheni, J. A.; Jenekhe, S. A. *J. Am. Chem. Soc.* **1995**, *117*, 7389. (j) Alam, M. M.; Jenekhe, S. A. *Chem. Mater.* **2002**, *14*, 4775. (k) Babel, A.; Jenekhe, S. A. *J. Phys. Chem. B* **2002**, *106*, 6129.
- (a) Wang, S.; Bao, G.; Wu, P.; Han, Z. *Eur. Polym. J.* **2000**, *36*, 1843. (b) Wang, S.; Bao, G.; Lu Z.; Wu, P.; Han, Z. *J. Mater. Sci.* **2000**, *35*, 5873. (c) Wang, S.; Wu, P.; Han, Z. *Polymer* **2001**, *42*, 217. (d) Wang, S.; Wu, P.; Han, Z. *Macromolecules* **2003**, *12*, 4567. (e) Wang, S.; Wu, P.; Han, Z. *J. Mater. Sci.* **2004**, *39*, 2717. (f) Wang, S.; Guo, P.; Wu, P.; Han, Z. *Macromolecules* **2004**, *37*, 3815. (g) Guo, P.; Wang, S.; Wu, P.; Han Z. *Polymer* **2004**, *45*, 1885. (h) Wang, S.; Lei, H.; Guo, P.; Wu, P.; Han, Z. *Eur. Polym. J.* **2004**, *40*, 1163. (i) Feng, D.; Wang, S.; Zhuang, Q.; Wu, P.; Han Z. *J. Mol. Struct.* **2004**, *707*, 169. (j) Feng, D.; Wang, S.; Zhuang, Q.; Wu, P.; Han Z. *Polymer* **2004**, *45*, 8871. (k) Guo, P.; Wang, S.; Lei, H.; Wu, P.; Han, Z. *Acta Polym. Sin.* **2005**, *1*, 86.
- Roncali, J. *Chem. Rev.* **1997**, *97*, 173.
- (a) Kitamura, C.; Tanaka, S.; Yamashita, Y. *Chem. Mater.* **1996**, *8*, 570. (b) Tachibana, M.; Tanaka, S.; Yamashita, Y.; Yoshizawa, K. *J. Phys. Chem. B* **2002**, *106*, 3549.
- Dotrong, M.; Mehta, R.; Balchin, G. A.; Tomlinson, R. C.; Sinsky, M.; Lee, C. Y.-C.; Evers, R. C. *J. Polym. Sci., Part A: Polym. Chem.* **1993**, *31*, 723.
- Promislow, J. H.; Preston, J.; Samulski, E. T. *Macromolecules* **1993**, *26*, 1793.
- (a) Jenekhe, S. A.; Johnson, P. O.; Agrawal, A. K. *Macromolecules* **1989**, *22*, 3216. (b) Jenekhe, S. A.; Johnson, P. O. *Macromolecules* **1990**, *23*, 4419.

- (10) Fratini, A. V.; Lenhert, P. G.; Resch, T. J.; Adams, W. W. *Mater. Res. Soc. Symp. Proc.* **1989**, *134*, 431.
- (11) (a) Donat-Bouillud, A.; Lévesque, I.; Tao, Y.; D'Iorio, M.; Beaupré, S.; Blondin, P.; Ranger, M.; Bouchard, J.; Leclerc, M. *Chem. Mater.* **2000**, *12*, 1931. (b) Leclerc, M. *J. Polym. Sci., Part A: Polym. Chem.* **2001**, *39*, 2867.
- (12) Brédas, J. L.; Silbey, R.; Boudreaus, D. S.; Chance, R. R. *J. Am. Chem. Soc.* **1983**, *105*, 6555.
- (13) (a) Hou, Q.; Niu, Y.; Yang, W.; Yang, R.; Yuan, M.; Cao, Y. *Acta Polym. Sin.* **2003**, *2*, 161. (b) Niu, Y. H.; Hou, Q.; Yuan, M.; Huang, J.; Cao, Y. *Chin. J. Lumin.* **2002**, *23*, 431. (c) Huang, J.; Niu, Y.; Yang, W.; Hou, Q.; Xu, Y.; Yuan, M.; Cao, Y. *Acta Chim. Sin.* **2003**, *61*, 765. (d) Huang, J.; Niu, Y.; Yang, W.; Mo, Y.; Yuan, M.; Cao, Y. *Macromolecules* **2002**, *35*, 6080.
- (14) (a) Klärner, G.; Lee, J.-I.; Davey, M. H.; Miller, R. D. *Adv. Mater.* **1999**, *11*, 115. (b) Lee, J.-I.; Klärner, G.; Davey, M. H.; Miller, R. D. *Synth. Met.* **1999**, *102*, 1087.
- (15) (a) Conwell, E. *Trends Polym. Sci.* **1997**, *5*, 218. (b) Schwartz, B. J. *Annu. Rev. Phys. Chem.* **2003**, *54*, 141. The existence of ground-state aggregates was verified by that substantial PL can be excited by 530 nm radiation where the absorption is essentially zero, as also discussed in refs 4d and 17.
- (16) (a) Chen, X. L.; Jenekhe, S. A. *Macromolecules* **1996**, *29*, 6189. (b) Chen, X. L.; Jenekhe, S. A. *Synth. Met.* **1997**, *85*, 1431. (c) Chen, X. L.; Jenekhe, S. A. *Appl. Phys. Lett.* **1997**, *70*, 487.
- (17) (a) Samuel, I. D. W.; Rumbles, G.; Collins, C. J. *Phys. Rev. B* **1995**, *52*, R11573. (b) Blatchford, J. W.; Gustafson, T. L.; Epstein, A. J.; Vanden Bout, D. A.; Kerimo, J.; Higgins, D. A.; Barbara, P. F.; Fu, D. K.; Swager, T. M.; MacDiarmid, A. G. *Phys. Rev. B* **1996**, *54*, R3683. (c) Blatchford, J. W.; Jesson, S. W.; Lin, L.-B.; Gustafson, T. L.; Fu, D. K.; Wang, H. L.; Swager, T. M.; MacDiarmid, A. G.; Epstein, A. J. *Phys. Rev. B* **1996**, *54*, 9180. (d) Lemmer, U.; Heun, S.; Mahr, R. F.; Scherf, U.; Hopmeier, M.; Siegner, U.; Gobel, E. O.; Mullen, K.; Bassler, H. *Chem. Phys. Lett.* **1995**, *240*, 373. (e) Nguyen, T.-Q.; Doan, V.; Schwartz, B. J. *J. Chem. Phys.* **1999**, *110*, 4068.

MA051516B